Accepted Manuscript

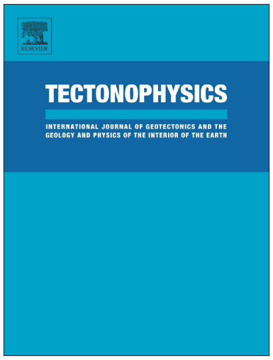

Tectonic evolution and extension at the Møre Margin – Offshore mid-Norway

S. Theissen-Krah, D. Zastrozhnov, M.M. Abdelmalak, D.W. Schmid, J.I. Faleide, L. Gernigon

PII: S0040-1951(17)30369-4
DOI: doi: 10.1016/j.tecto.2017.09.009
Reference: TECTO 127622

To appear in: *Tectonophysics*

Received date: 3 March 2017
Revised date: 8 September 2017
Accepted date: 12 September 2017

Please cite this article as: S. Theissen-Krah, D. Zastrozhnov, M.M. Abdelmalak, D.W. Schmid, J.I. Faleide, L. Gernigon , Tectonic evolution and extension at the Møre Margin – Offshore mid-Norway, *Tectonophysics* (2017), doi: 10.1016/j.tecto.2017.09.009

Tectonic evolution and extension at the Møre Margin – offshore mid-Norway

S. Theissen-Krah[1)2)], D. Zastrozhnov[2)3)], M. M. Abdelmalak[2)3)], D. W. Schmid[4)], J. I. Faleide[2)], L. Gernigon[5)]

[1)] GEOMAR Helmholtz Centre for Ocean Research Kiel, Wischhofstr. 1-3, 24148 Kiel, Germany

[2)]Centre for Earth Evolution and Dynamics (CEED), University of Oslo, Norway

[3)]Volcanic Basin Petroleum Research (VBPR), Oslo Science Park, 0349 Oslo, Norway

[4)]Physics of Geological Processes (PGP), University of Oslo, Norway

[5)] Geological Survey of Norway (NGU), Leiv Erikssons vei, 39 Trondheim, Norway

Abstract

Lithospheric stretching is the key process in forming extensional sedimentary basins at passive rifted margins. This study explores the stretching factors, resulting extension, and structural evolution of the Møre segment on the Mid-Norwegian continental margin. Based on the interpretation of new and reprocessed high-quality seismic, we present updated structural maps of the Møre margin that show very thick post-rift sediments in the central Møre Basin and extensive sill intrusion into the Cretaceous sediments. A major shift in subsidence and deposition occurred during mid-Cretaceous. One transect across the Møre continental margin from the Slørebotn Subbasin to the continent-ocean boundary is reconstructed using the basin modelling software TecMod. We test different initial crustal configurations and rifting events and compare our structural reconstruction results to stretching factors derived both from crustal thinning and the classical backstripping/decompaction approach. Seismic interpretation in combination with structural reconstruction modelling does not support the lower crustal bodies as exhumed and serpentinised mantle. Our extension estimate along this transect is ~188 ± 28 km for initial crustal thickness varying between 30 and 40 km.

Keywords: basin modelling, Stratigraphy reconstruction, Møre continental margin, Extension, Stretching Factors

Introduction

The Møre Margin is a segment of the Mid-Norwegian passive continental margin and is located between 62° and 65 °N and 0° and 6° E (Fig. 1). It is separated from the Vøring Margin by the Jan Mayen Corridor in the north and by the north-westward extension of the Tampen Spur from the Magnus Basin in the south. The Møre continental margin comprises of the deep sedimentary Møre Basin, which is bounded to the Møre Marginal High by the Faroe-Shetland-Escarpment to the west and the Møre Trøndelag Fault Complex to the east. The Møre Margin is divided into several sub-basins and highs (Fig. 1) and includes the Møre Trøndelag Fault Complex and the Slørebotn Subbasin in the east.

The Mid-Norwegian margin has been studied extensively for hydrocarbon exploration and consequently large amounts of seismic data have been acquired. Many studies that address similar stretching and extension estimates focused on the Vøring Margin (e.g. Gernigon et al., 2003; Reemst and Cloetingh, 2000; Theissen and Rüpke, 2010; Wangen and Faleide, 2008; Wangen et al., 2011). However few studies address the Møre continental margin segment specifically (Gabrielsen et al., 1999; Gomez et al., 2004; Skogseid et al., 2000). This study focuses on stretching factors and extension along a seismic profile crossing the entire Møre continental margin. We further discuss the implication of different modelling approaches, seismic interpretation, rifting events, and initially assumed crustal configuration. The modelling tool TecMod and the classical backstripping/decompaction method are used to reconstruct the stratigraphy and calculate stretching and extension. The stretching factor (beta) is compared to estimates from crustal thinning, where beta is estimated by dividing the assumed initial crustal thickness prior to rifting by the today's thickness.

Geological Setting

The Mid-Norwegian margin developed through several rift episodes since the collapse of the Caledonides in the Devonian. The final rift phase during the Upper Cretaceous eventually led to breakup between Greenland and Eurasia in the Eocene (Talwani and Eldholm, 1972).

Several early rift phases during Late Palaeozoic-Early Mesozoic have been suggested for the Norwegian-Greenland rift system (Grunnaleite and Gabrielsen, 1995). The earliest rift episode that can be observed in the seismic sedimentary strata at the Mid-Norwegian margin is Permian-Triassic in age. Evidence for this event has been described at the Trøndelag Platform and the Halten Terrace (Tsikalas et al., 2012). During this early rift phase Caledonian basement trends were reactivated and rifting was oriented ENE-WSW (Gomez et al., 2004).

The major rift event during which the crust was highly thinned took place during Late Jurassic - Early Cretaceous and was mainly non-magmatic (Brekke, 2000) with minor magmatic activity suggested by evidence for Cretaceous seamounts and the presence of pyroclastic rocks (Lundin and Dore, 1997) in the Vøring Basin. Both tectonic and thermal subsidence during the Cretaceous led to the accumulation of up to 8 km of sediments in local depocentres in the Vøring and Møre basins (Scheck-Wenderoth et al., 2007). The extension direction during Late Jurassic-Early Cretaceous shifted to a NW-SE direction and the final opening occurred almost perpendicular to the present day coastline (Doré et al., 1999; Mosar et al., 2002). A separate rift event during the mid-Cretaceous is debated; Grunnaleite and Gabrielsen (1995) suggest a mid-Cretaceous rift event, while other studies conclude that no stretching occurred during the mid-Cretaceous (Faerseth and Lien, 2002).

A last stretching event during Late Cretaceous-Palaeocene is constrained by seismic data from the Vøring margin and it has been suggested that the main rift event was initiated during Late Maastrichtian (Ren et al., 1998) or mid-Campanian time (Gernigon et al., 2003; Ren et al., 2003). The Campanian-Palaeocene rifting is less pronounced in seismic data from the Møre Margin, but evidence for brittle deformation is observed close to the Tertiary lava flows. Final lithospheric separation was accompanied by voluminous magmatism resulting in numerous sill intrusions, lava flows and characteristic seaward dipping reflectors (SDR), that cover large areas towards and over the continent-ocean boundary (COB) (Berndt et al., 2001; Planke et al., 2005; Ren et al., 2003 and Fig. 1). Breakup was initiated during the Palaeocene-Eocene transition (C24r, (Gernigon et al., 2012)) .

Lower crustal bodies (LCBs) with high P-wave velocities (>7km/s) are characteristic for the outer parts of the Mid-Norwegian margin. LCBs occur below or are part of the lower crust and are observed beneath the marginal highs and the volcanic provinces. They continue to the east below the stretched and thinned crust of the deep Vøring and Møre basins. The LCBs have been imaged in most of the parts of the Møre Basin and are described to be 2-5 km thick with thickening beneath the intra basinal highs (Faleide et al., 2008; Kvarven et al., 2014; Lundin and Dore, 2011; Mjelde et al., 2009). Traditionally the LCBs in the outer part of the Møre and Vøring margins have been interpreted as breakup related magmatic underplating (Mjelde et al., 2009; Olafsson et al., 1992; White and McKenzie, 1989), but alternative magmatic and non-magmatic origins (e.g. a post Caledonian metamorphic core complex, a sill complex intruded into the lower crust or serpentinised mantle rocks) have been suggested and discussed (Dore et al., 1997; Gernigon et al., 2006; Gernigon et al., 2004; Osmundsen and Ebbing, 2008; Reynisson et al., 2010). The concept of mantle serpentinisation during continental rifting is based on the observations from the non-volcanic Iberian margin (Perez-

Gussinye et al., 2001) and similar processes have been suggested for the inner parts of the LCB at the Norwegian margin (Lundin and Dore, 2011). Prerequisite for serpentinisation is a complete embrittlement of the crust and the presence of fluids. Rüpke et al. (2013) showed that despite the thick sedimentary cover that lead to higher temperatures in the lower crust compared to basin with thin sediment thicknesses, serpentinisation is possible above a critical stretching factor. The critical stretching factor depends on sedimentation rate and rift duration, but is generally high, e.g. above 6 for an average sedimentation rate of 0.2 mm/yr. The nature and origin of the LCB and in particular the question if serpentinisation can effectively occur at volcanic (and rifted) passive margins, and to what extent a comparison between volcanic and non-volcanic margins is valid (Péron-Pinvidic et al., 2013) or not (Geoffroy et al., 2015; Gernigon et al., 2015), is an ongoing debate.

Seismic Interpretation

The study area comprises approximately 600 new and reprocessed seismic reflection and refraction data. The key seismic reflection lines cross the Møre Basin in northwest-southeast direction approximately perpendicular to the line of breakup. The main tectonic features are well imaged by the seismic data set, including several intra-basinal highs (Grip High, Vigra High, Ona High and Giske High), and the Slørebotn Subbasin. The southern extensions of the Modgunn Arch and Ormen Lange Dome are imaged in the northern part of the study area (Fig. 1b, Fig. 2, and Fig.3).

Structures and sedimentary layering are well recognised in the south-eastern part of the Møre Basin, whereas interpretation of the north-western part is hindered by numerous sill intrusions and lava flows close to the COB. The sedimentary units were tied to wells available in the Møre and southern Vøring area (Fig. 1b). Data of the deeper parts of the Møre Basin are limited and only 5 wells are drilled through Late Cretaceous or older formations, two of which are located in the Slørebotn Subbasin. The depth to the basement is therefore difficult to constrain in some parts of the area, and earlier studies define the depth of the Møre Basin to be the base Cretaceous level (Blystad et al., 1995). The new and reprocessed data set allows better interpretation of the depth to the basement in the proximal part of the margin. In the distal domain we used the lithosphere model from Scheck-Wenderoth and Maystrenko (2008) for the interpretation of the top basement.

Most of the seismic sections show the existence of thick sedimentary strata below the base Cretaceous reflection down to the recorded depth of 10 s TWT. The ages of this succession remain unknown since the base Cretaceous has never been drilled in the deep Møre Basin, but it is likely that these sediments correlate to the pre-Cretaceous sequences that have been drilled on the platforms and in the Slørebotn Subbasin.

A strong reflector within the Cretaceous sequence interpreted to be of intra-Cenomanian age can be followed on all seismic profiles in the study area. The depth to this reflector is about 5.5 to 6 s TWT in the central part of the basin (Fig. 2). Another prominent reflector interpreted as the base Cretaceous unconformity (BCU), defines Jurassic-Cretaceous syn-rift to post-rift transition reaches depth to 8 s TWT in the deep basins. This reflection is however not as distinct on all profiles as the intra-Cenomanian and different interpretations are possible (Grunnaleite and Gabrielsen, 1995). In addition to the intra-Cretaceous and the base Cretaceous marker, the reflection corresponding to the Top Cretaceous level has been identified on all profiles, which allows us to estimate the thickness of the Cretaceous sequence in the entire Møre Basin (Fig. 2).

The present-day relief of the BCU is shown in Fig. 2a. The BCU is deepest, up to 8s TWT on the western flank of the major structural highs and faults in the central basin (e.g. Vigra High, Grip High, Slettringen Ridge). The BCU shallows again towards the COB, which is also expressed in the Møre Marginal Plateau, a shallow platform, which can be interpreted as a northern continuation of the Faroe Platform. As suggested by Gernigon et al. (2015) this shallow platform (Møre Marginal Plateau) could represent a continental and marginal plateau that existed prior to continental breakup. In this case the plateau can be directly related to the prolongation of the Jan Mayen Microcontinent (JMMC) which was initially part of the Møre Basin between the Faroe Platform and the outer Vøring Basin (Gaina et al., 2009; Gernigon et al., 2012). From potential field modelling and the resulting pre-drift configuration, Gernigon et al. (2015) suggested that Mesozoic and possibly Palaeozoic sediments could be present beneath the outer Møre Margin and underneath a large part of the Møre Basin.

The mid-Cenomanian map represents the basin configuration after ~ 40 m.y. of syn-rift. The depth to this reflector increases from the Slørebotn Subbasin towards the central Møre Basin with maximum depth of 6-6.5 s TWT west of the Vigra and Grip highs, and shallows again towards the Møre Marginal High. Mid-Cenomanian reflector is absent on the Manet Ridge, Frøya High and in the western part of the Halten Terrace. The deepening of this reflector west of Vigra and Grip high, and the Slettringen Ridge is comparable to the BCU map (Fig. 2a). In contrast to the configuration at the base Cretaceous, the deepening of the Mid-Cenomanian reflector extends further to the west in the central parts and towards the COB. This subsidence suggests that minor faulting occurred during that time, probably due to reactivation of the old fault systems.

The Top Cretaceous (Fig. 2c) map shows a different pattern with a rather uniform depth except the prominent low in central basin and along the margin (Fig. 2b). Thick lava flows covering the western margin and post-breakup thermal subsidence is likely to have caused the deepening of the Top Cretaceous layer at the margin close to the COB. In the northern part (Møre-Vøring transition) the Top Cretaceous level seems to thin slightly towards the COB. Glacial loading and the corresponding high sedimentation rates have probably caused further subsidence seen in the central part.

The Late Cretaceous sediments are affected by the formation of domes during the Mid-Miocene compression (Grunnaleite and Gabrielsen, 1995; Lundin and Dore, 2002) and are distinct features on the Mid-Cenomanian (Ormen Lange dome, Isaak dome, Helland Hansen Arch) and Top Cretaceous time-structure maps (Fig. 2b,c).

Figures 2 d-f show the cumulative sediment thickness of the Cretaceous units and the evolution of the depocenters in the Early and Late Cretaceous. Several depocenters, up to 6 s TWT thicknesses, trending NNW-SSE are observed along the western flanks of major faults.

Two prominent depocenters with up to 6.3 s thickness are present, one in the southern part of the central Møre Basin and a second depocenter that is located in the northern part at the transition to the Vøring Basin (southern Rås Basin). The comparison of the thickness distribution of the upper and Lower Cretaceous reveals a major shift in depositional environment during the mid-Cretaceous. The depocenters that were initiated during the main rift event in the Jurassic/Cretaceous are filled with thick Lower Cretaceous sediments (Fig. 2e). Very thin or absent Lower Cretaceous strata (e.g. Vigra, Ona, and Frøya High) is probably caused by non-deposition and/or erosion due to footwall uplift and rotation of the central and continental rafts preserved in the deep part of the Cretaceous Møre Basins.

The thickness distribution of the Upper Cretaceous (Fig. 2d) shows a different pattern with nearly uniform sediment thickness in the central Møre Basin. Subsidence and significantly higher sedimentation occur in the northern part towards the transition to the Vøring Basin, which suggests different tectonic environments in the Møre Basin during the Late Cretaceous with only minor tectonic activity at the Møre margin.

Using average interval velocities proposed by Scheck-Wenderoth et al. (2007) for layer depth conversion allows thickness and depth estimates for the different sedimentary units. The Cenozoic succession is around 2 km thick in the Slørebotn Subbasin and increases to a maximum depth of over 4 km west of Vigra High. The base of the Upper Cretaceous reaches its maximum with 7.6 km in the sag basin between the Vigra and Grip highs. In average the central Møre Basin consists of 3 to more than 4 km of Upper Cretaceous sedimentary strata.

Our data agree with previous interpretations that the Møre Basin is a deep sedimentary basin with thick Cretaceous sequence (e.g. Gomez et al., 2004). Particularly in the depocenters on either side of Vigra High thick sedimentary wedges are imaged down to 10 s TWT (corresponding to depths of 15-16 km). Additionally the new seismic data suggest, that the Møre Margin also contains thicker layers of possibly pre-Cretaceous strata and not shallow basement or an outer zone of exhumed continental mantle as suggested by (Peron-Pinvidic et al., 2013).

Modelling

We use the basin modelling software TecMod (Rüpke et al., 2008) for the reconstruction of the Møre transect. TecMod couples a forward model to an inverse modelling algorithm to fit a specific basin stratigraphy. The forward model is based on pure-shear kinematics and resolves for basin scale, e.g. sedimentation and compaction, and lithosphere processes, such as rifting, heat transfer, and flexural isostasy on a Lagrangian finite-element mesh. The advantage of this reconstruction is that in each time step, new sediment packages are deposited to be part of the computational domain for the following time steps. The sediments are therefore included in the thermal calculations to account for thermal blanketing effects which may lead to considerable differences in heat flow and subsidence history compared to the results of method that decouple both thermal and structural processes (Theissen and Rüpke, 2010; Wangen, 1995). During the inversion the stretching factors and palaeo-water depths values are iteratively updated until the forward modelling results match the observed input stratigraphy. During the fitting process only the thickness and the location of sediment packages are used to update the forward parameters and well data such as present-day temperature, vitrinite reflectance data and estimates of palaeo-water depth can therefore be used to verify the corresponding model results. Further details of the automated basin reconstruction method are described in Rüpke et al. (2008; 2010).

Møre Transect

Our key profile across the Møre margin consists of a new TGS seismic line (Fig. 3a) and line M-M' (MB-6-92) in Blystad et al. (1995) to the southeast. Figure 3b shows our geological interpretation of the Møre profile. The seismic line LOS 99-002 overlaps with this transect for ~25 km and runs from the Møre Marginal High to the extinct Aegir Ridge (Fig. 4). The deep crustal interpretation for this part of the profile is taken from Breivik et al. (2006).

The transect runs from the continental shelf to the Møre Marginal High and images the sedimentary strata in the Møre Basin and the typical lava flows and SDR approaching the continent-ocean boundary in the northeast. This profile can be subdivided into structural highs separating the sedimentary depocentres from southeast to northwest, these are: Giske High, Ona High and Vigra High. In addition to the main highs the new data show narrow and deep sub-basins, each of around 10 km width and up to 14 km deep between the Vigra and Ona highs. Small basins bounded by rotated fault blocks can be identified in the northeast whereas the normal faults dip mainly towards northwest. Several sill intrusions within the Lower Cretaceous sequence are present between km 100-150 (Fig. 3a). The eastern part the Møre Basin displays a basin shape with sedimentary sequences dipping to the east, whereas in the western part the Upper Cretaceous and Cenozoic sequences run nearly horizontal towards the Møre Marginal High.

In contrast to previous interpretations (Faerseth and Lien, 2002; Gomez et al., 2004) which describe no evidence for tectonic activity in the Cretaceous, we observe normal faults in the western part of the transect that cut at least through the lowermost Cretaceous sediments, suggesting rifting or tectonic activity during Early Cretaceous time. As mentioned above large areas approaching the COB are covered with lava flows and sill intrusions, which makes interpretation of the western part of the profile difficult (0-70 km). Our interpretation in this part agrees well with published interpretation mainly based on wide-angle seismic data (Faleide et al., 2008; Kvarven et al., 2014; Nirrengarten et al., 2014).

Model setup

Two sets of models are investigated. The first set focuses on the structural evolution of the Møre Basin (Fig. 3), while in the second the whole transect to the Aegir Ridge (Fig. 4) is reconstructed to investigate the impact of the breakup and spreading in the modelling.

Commonly used pre-rift crustal thicknesses for the Norwegian margin are between 30 and 40 km (Gernigon et al., 2006; Rüpke et al., 2013; Theissen and Rüpke, 2010; Wangen and Faleide, 2008). The choice of the initial crustal thickness influences the stretching factors necessary to create a sedimentary basin of a given depth and we therefore investigate the effect of different initial crustal thicknesses, i.e. 30 to 40 km. All input parameters and material properties are listed in table 1. Additionally we introduce initial crustal heterogeneities and lower crustal bodies at various locations to fit the observed gravity and OBS data. The details of these models are described in the gravity section below. We assume the following three rift phases for our reference setup:

(1) Permian/Early Triassic rifting from 270-250 Ma to account for the early stretching episodes, prior to the main phase during
(2) Late Jurassic/earliest Cretaceous (170-145 Ma).
(3) A final rift phase starting in Late Cretaceous (80Ma) until breakup at 55 Ma.

We also test a longer second rift phase extending until Aptian time (115 Ma), which is observed at the central and outer Vøring Margin. Due to the number of and ages applied to the sedimentary layers in our stratigraphy this alternative scenario leads to a Jurassic/Cretaceous rift phase from 170 – 115 Ma.

The temperature is fixed to 5°C at the seafloor and 1300°C at the boundary between lithosphere and asthenosphere. The lithosphere-asthenosphere boundary is considered to be the isostatic compensation depth and is at 125 km in all model setups. Radiogenic heat production in the crystalline crust exponentially decreases (e-fold length = 20 km) with depth from 2µW/m³ in the upper crust and 0.18µW/m³ in the lower crust. The effective sediment conductivities are computed as the geometric average between matrix and pore fluid conductivities.

Serpentinisation can potentially occur in all our model setups. The requirement is that high stretching leads to a complete embrittlement of the crust (Rüpke et al., 2013), which allows us to test if the LCB observed along the Møre profile could be serpentinised mantle and how the initial configuration influences the possibility of serpentine formation.

The second setup is the extended profile shown in figure 4 that runs to the Aegir Ridge and the reconstruction focus on the extension of the Norwegian part of the Norway-Greenland rift system. Material properties, rift phases and initial crustal thicknesses described above are the same in both setups. Breakup at 55 Ma is included and spreading in the Norway Basin is active until 28 Ma and produces 9 km thick oceanic crust. All models assume flexural isostasy with a necking depth of 15 km and an effective elastic thickness of 5 km.

Gravity Modelling

Gravity modelling is performed to test different interpretation and possible locations of the known LCBs that are used as input parameter for the reconstruction modelling. TecMod´s gravity modelling is based on the computation of the gravitational acceleration due to a 2-

dimensional body described by Talwani et al. (1959) and the reformulated algorithm by Won and Bevis (1987).

TecMod's finite-element mesh is used to calculate the gravity anomalies. This method allows for computing the changes in gravity anomaly along a reconstructed profile, which can then be compared to measured gravity anomaly changes. We compare observed free-air gravity anomaly data provided by TGS, which are comparable to the Word Gravity Map (WGM2012) that is freely available from the Bureau Gravimétrique International (BGI) http://bgi.omp.obs-mip.fr/ (The International Gravimetric Bureau, 2012) with our modelling results for the profile across the Møre Basin (Fig. 3).

The gravity comparison consists of three steps of modelling: (1) the profile (Fig. 3b) is reconstructed with TecMod as described above to compute the necessary stretching factors to create the Møre Basin. This setup does not include any initial heterogeneities or lower crustal bodies. (2) The actual gravity comparison is performed with TecMod's forward modelling scheme due to the faster computation compared to the reconstruction. Stretching factors resulting from step 1 are used as input parameters. In this step we introduce high-density bodies to mimic the lower crustal body. The initial heterogeneities together with the LCBs give a close match with the observed gravity anomalies. In the last step (3), we run again the full basin reconstruction including the LCB and the heterogeneous initial crust to verify the results from the initial reconstruction. We test different densities and locations for an inner and outer LCB based on our interpretation and suggested in various publications (e.g. Kvarven et al., 2014; Nirrengarten et al., 2014). The density is 3300 kg/m^3 and 3100 kg/m^3 for the inner and outer LCB, respectively. With this assumption we do not specify the nature of the LCBs, but the LBCs are treated as crustal heterogeneities. In an alternative setup the outer

LCB is treated as magmatic underplate coming into the model at 55Ma. Additionally, it is assumed that the tectonic evolution at the Norwegian margin before mid-Permian (the starting age in our model) led to a heterogeneous crust where the initial thicknesses of the upper and lower crust vary horizontally. It should be noted that the heterogeneities and the LCBs do not change the total initial crustal thickness; it changes the density distribution throughout the crust due to varying proportions of upper and lower crust, and the implemented higher density LCBs/underplate. The total initial thickness is varied between 30 and 40 km.

The best fit of the gravity data is achieved with an inner LCB between 565 and 615 km with a maximum thickness of 4.5 km was needed to fit the gravity observations in the south-eastern part of the transect (Fig. 5). The outer LCB or alternatively magmatic underplating occurs from the north-western start of the profile to the intrabasinal low between Vigra and Ona High. A thicker magmatic underplate is needed to fit the gravity data, compared to the outer LCB as part of the lower crust.

Modelling Results

Stratigraphy, well comparison and crustal configuration

All reconstructions were run for 30 iterations and the input stratigraphy is fitted well for all models. To calibrate the results we compare computed temperature and maturity with available measurements from wells (Fig. 6). Vitrinite reflectance data (%Ro, Sweeney and Burnham (1990)) as indicator for maturity is sensitive to the temperature-time evolution and therefore well suited to verify the thermal solution of the reconstruction. For four wells temperature and vitrinite reflectance data were available: well 6302/6-1 and well 6403/10-1 in the Møre Basin are located ca. 30 south and 24 km north of the transect, respectively. The other two boreholes are also ca. 30 km north of the profile and have been drilled in the

Slørebotn Subbasin, which can explain the local mismatch in temperature data. Nevertheless the overall computed temperature and maturity data match the present-day measurements well (Fig. 6), which confirms that the modelled thermal evolution (temperature and heat flow through time) provide valid solutions and it constrains the thermal parameter choice (radiogenic heat production, sediment conductivities).

In addition to the stratigraphy comparison we compare the computed crustal configuration with results inferred from our seismic data and potential field modelling (Faleide et al., 2008; Kvarven et al., 2014; Nirrengarten et al., 2014). At the end of the reconstruction the crust in the central basin is considerably thinned. The best fit is achieved with initially 32-35 km thick crust, also regarding the depth of the Moho, which lies in 20 km depth beneath the sag basins in the centre and shallows to ~17 km towards the north-western end of the profile (Fig. 5).

Although the reconstruction only aims at matching the basin stratigraphy by pure shear deformation without considering faults in the crust, the resulting crustal thicknesses and Moho depth are comparable to interpretations from potential field modelling and wide-angle seismic data. The discrepancies in LCB thickness are also due to the modelling focus on sedimentary basin reconstruction, but as shown below, the consideration of such heterogeneities is important for the calculation of stretching factors and therefore the estimation of extension at continental margins.

Stretching Factors and Extension

The second (breakup) setup is used to investigate stretching factors between Norway and the Aegir Ridge. The stretching factors calculated by the stratigraphy reconstruction are shown in Fig. 7. Figure 7a shows the cumulative crustal stretching factor and stretching factors for each rift phases for an initial crustal thickness of 35 km. High stretching occurs at the deepest depocentres, e.g. on either side of the Vigra High with a maximum stretching factor $\beta = 3.3$ in the centre of the basin after three periods of rifting. The highest thinning factors are computed in the north-western part at the breakup location, but it should be noted that the depth of the depocenter here is not well resolved due to the overlying volcanics. Stretching decreases towards the southeast with beta factors below 2. Major thinning took place during the first two rift episodes between Triassic and Early Cretaceous. The final rift phase that eventually led to breakup accounts only for ~35 % of lithospheric stretching.

Assuming an initial crustal thickness of only 30 km the average β-factor is higher (3.9) with maximum values of 5 in the deep sub-basins. Lower values are computed for a thicker initial crustal thickness of 40 km, 2.2 and 2.7 for average and maximum stretching, respectively (Fig. 7b). Including LCBs as magmatic underplate or initial heterogeneities requires higher stretching factors compared to models that do not include any heterogeneities in the crust (Fig. 7b).

The computed stretching factors required to fit the input stratigraphy of all setups are lower than the critical value to favour brittle deformation and hence serpentinisation.

In the setup that includes the extended Cretaceous rift phase yield the same total stretching factors, only the distribution is different. Compared to the models where stretching ceased in the Early Cretaceous, these setups show slightly less stretching during the last and final rift event, but higher beta factors during the Jurassic/Cretaceous (170-115 Ma) rift phase.

Crustal extension can be calculated by integrating crustal thinning (γ) along the profile length, where crustal thinning is defined by $\gamma = 1 - \frac{1}{\beta}$. The resulting extension is 188 ± 28 km (215 for 30 km crust and 160 for 40 km crust) for the models with an initial crustal thickness of 30-40 km.

Discussion

The results from new and reprocessed seismic data allow for detailed mapping of the Cretaceous and Cenozoic sedimentary successions in the Møre Basin. The major rift event during Jurassic/Early Cretaceous created several deep depocenters along the Møre Margin that are filled with thick Cretaceous and underlain by pre-Cretaceous sediments. The clear shallowing of the Base Cretaceous unconformity towards the Møre Marginal High and the shallow platform (Møre Marginal Plateau) highlighted by the new seismic data suggest that the crust is moderately thinned and that crustal fragments are still preserved and probably too thick to favour both mantle exhumation and serpentinisation to occur, which is in agreement with recent results from potential field modelling (Gernigon et al., 2015; Nirrengarten et al., 2014). Our stratigraphy reconstruction of the Møre transect supports this interpretation with a final crustal thicknesses of minimum 5-8 km (>10 km in the vicinity of the inner LCB) and no serpentine formation. This result is in contrast to the suggestion that the inner LCB could represent serpentinised mantle (Lundin and Dore, 2011; Rüpke et al., 2013) because our seismic interpretation and stratigraphy calibration is different compared to those studies. The location of the outer LCB seems to correlate to the location of sill intrusions (Abdelmalak et al., in prep) and we therefore prefer an interpretation for the outer LCB as magmatic underplate or magmatic intrusion into the preserved lower crust.

The thickness distribution of the Upper and Lower Cretaceous units (Fig. 3e,f) reveal that subsidence and sediment deposition shifted northwards towards the outer Vøring Margin after Cenomanian. The Møre Basin experienced subsidence and sedimentation mainly during the Early Cretaceous and less tectonic activity in Late Cretaceous, comparable to the observation by Scheck-Wenderoth et al. (2007), who suggested that fault activity is reduced in the Møre Basin during Late Cretaceous.

A comparison with previously published stretching factors and extension estimates is difficult because most studies focus only on post middle Jurassic rifting. Gomez et al. (2004) and Skogseid et al. (2000) estimated stretching and extension for the Møre margin by crustal thinning. Gomez et al. (2004) used only the upper crust for reconstruction and their results highly depend on the assumed pre-Cretaceous crustal thickness, i.e. the crustal thickness after earlier stretching episodes and it requires proper identification of the Base Cretaceous sediments and basement rocks. In the preferred model of Gomez et al. (2004) the pre-Cretaceous rift crustal thickness is already thinned to 20 km during earlier stretching episodes. Both studies suggest an extension of ca. 140-150 km since the middle Jurassic, which is comparable to the results of this study. However the distribution of extension is different, the final rift phase in our study only accounts for ca. 35 %, which corresponds to ca. 60 km, whereas Skogseid et al. (2000) suggested 87 km for Maastrichtian/Palaeocene rifting and in an earlier study calculated an extension of 90 to 111 km during Late Cretaceous/Palaeocene (Skogseid, 1994).

Roberts et al. (2009) proposed increasing stretching factors from 1 (unstretched) at the Mid-Norwegian margin to up to 4 at the Møre Marginal High for breakup related stretching during Palaeocene from flexural backstripping. They assumed an average $\beta = 1.4$ for the Base

Cretaceous. A study (Rüpke et al., 2013) using the same modelling approach, but different seismic data suggests very high stretching (β>8) for the deep sub-basins for the rift phase(s) prior to breakup related stretching. Our cumulative β (maximum 5 for 30 km crust) for these rift events is lower because we assume slightly shallower basins and apply the onset of the last rift phase during mid-Late Cretaceous and therefore do not need to create all the accommodation space for the Cretaceous sediments already during the Jurassic rift phase.

The determination of stretching factors and therefore also the estimated extension is not only dependent on the accuracy of geological interpretation, e.g. stratigraphy, crustal thickness or the assumed initial crustal thickness, but also highly affected by the method used to determine the stretching factors.

Figure 8 shows a comparison of total stretching factors for the Møre transect calculated with three different methods for an initial crustal thickness of 35 km: the classical backstripping and decompaction approach (Steckler and Watts, 1978), stretching estimated by crustal thinning, and the computed β-factors from the reconstruction modelling. In the backstripping approach individual sediment packages are consecutively decompacted to recover the subsidence history (Steckler and Watts, 1978) and the stretching factors can be calculated from the resulting tectonic subsidence (Stewart et al., 2000):

$$\beta^{-1} = 1 - \frac{S_{tec}(\rho_m - \rho_w)}{t_{c0}(\rho_m - \rho_c)}, \tag{1}$$

where S_{tec} are total tectonic subsidence, t_{c0} the initial crustal thickness prior to rifting, and ρ_m, ρ_w, and ρ_c are densities of the mantle, water, and crust, respectively. Stretching factors derived from the subsidence analyses are usually lower and are likely to be underestimated because stretching/thinning of the sediments is not included (Theissen and Rüpke, 2010; Wangen and

Faleide, 2008). In our case the calculated sediment thicknesses are up to 50-60% lower for certain sediment packages (e.g. between 115 and 145 Ma) if the sediments are only backstripped and decompacted but not thinned during the formation of the basin, compared to the reconstruction modelling where thinning of the sediments is included. Crustal stretching inferred by crustal thinning is poorly constrained because only the initial thickness is compared to the crustal thickness observed today and both values itself are subjected to large uncertainties. This method does not include any fault reconstruction or area balancing and often gives large discrepancies if compared to other methods (Ranero and Perez-Gussinye, 2010). The stretching factors are higher compared to the reconstruction modelling due to the thicker crust at the end of the reconstruction compared to what has been observed. Despite the discrepancies in crustal configuration and thickness of the LCB's between the our modelling results and the initial seismic interpretation the influence of implementing LCBs is seen in the computed stretching factors with higher stretching required in models that include crustal heterogeneities.

By applying an initial crustal thickness of 32-35 km thickness, compared to the even thicker (~40 km) crust observed close to the Norwegian mainland (Kvarven et al., 2014), we assume that the crust has already been partly thinned during the episodes of stretching prior to the Permian/Early Triassic rift phase. Despite all research, also driven by the hydrocarbon industry the mechanism that leads to highly thinned crust is not fully understood. Osmundsen and Ebbing (2008) suggested that the crust is thinned along large low-angle detachment faults that thin the crust from initial thicknesses of up to 40 km to less than 10 km. This mechanism is compared to the 'thinning mode' (Lavier and Manatschal, 2006) derived from the Iberian margin. Although we do not see large basin flank detachment fault in our profiles across the Møre Basin it is possible that low-angle normal faults play an important role in thinning the crust but are in our case overprinted by the thick sedimentary cover and sill complexes. This is also in agreement with Lavier and Manatschal (2006) who describe that the thinning mode often affects parts of the margin that are usually buried under thick sediments. However, we also find a comparison with the Iberian margin difficult because the major rift phase during Late Jurassic/Early Cretaceous, responsible for the highly thinned crust, most likely aborted during mid-Cretaceous and was not a continuous process leading to the Eocene breakup. An alternative model to stretch the crust has been suggested by Ranero and Pérez-Gussinye (2010) who showed that very high thinning of the crust can be explained by normal faulting if the faults are active sequentially in time.

In plate reconstruction studies extension is quantified by the overlap of the continent-ocean boundary and has been estimated to be ~400 km between Greenland and the mid-Norwegian margin, which corresponds to an average stretching factor of at least 2 (Torsvik and Cocks, 2005; Torsvik et al., 2001). Using recently published rift velocity (Brune et al., 2016) the total extension between Greenland and Norway at the location of our transect of ~440 km between 200 Ma and breakup. Our model data fit with the proposed stretching estimates derived from plate reconstruction studies (Brune et al., 2016; Torsvik et al., 2001), if we assume that about half the extension between the Norway and East Greenland takes place at the Møre Margin and the other half is distributed between the Jan Mayen Microcontinent and the conjugate East Greenland Margin.

Very high stretching factors of about 4-5 (maybe locally higher) characterize the deepest sub-basin. A more precise estimation of stretching and extension derived from stratigraphy reconstruction is only possible if sub-volcanic imaging/interpretation is improved and if deeper well data allow for better age constraints.

Conclusions

New and reprocessed seismic data from the Norwegian passive margin allow for better interpretation of the seismic stratigraphy in the central Møre Basin. To derive stretching and extension that occurred during several episodes of rifting we have reconstructed the Møre Basin using different methods. Gravity modelling supports two LCBs along the transect and suggests the existence of heterogeneous thickness of the upper and lower crust prior to the first applied stretching event during Permian/lower Triassic.

The reconstruction study fits well the present-day stratigraphy, temperature, and maturity data derived from boreholes. The key points of our study are:

- The central Møre Basin is a deep basin with thick post-rift sedimentary strata following the main rift episode during Late Jurassic/Early Cretaceous. The sedimentary infill has locally maximum depth of 10 s TWT (corresponding to 15-16 km). Cretaceous depocenters are concentrated along the western flank of the structural highs. A major shift of subsidence and deposition to the north towards the Møre-Vøring transition occurred during mid-Cretaceous.
- The estimation of extension highly depends on the method. Compared to the reconstruction modelling, stretching evaluated by crustal thinning gives very high values, while the classical backstripping approach yields lower beta factors due to the underestimation of sedimentation. Up to ~60 % more sedimentary infill is necessary if the sediments are also stretched during reconstruction of the present-day stratigraphy. This leads to higher stretching factors compared to the decompaction/backstripping calculations.
- Our result does not support the interpretation of the LCBs as serpentinised mantle along most of the reconstructed profile. The observed and modelled crustal remains

too thick for complete mantle exhumation and high rate of serpentinisation required to explain the P-waves values of the LCB. We prefer a model where the outer LCB is related to magmatic intrusion into the pre-existing inherited lower crust and/or magmatic underplating.

- The extension along the reconstructed profile across the Møre Basin is estimated to 188 ± 28 km. It is comparable to estimations from plate reconstruction studies. The main thinning phase occurred before the final and separate rift episode leading to breakup.

Acknowledgment

This work is part of the project OMNIS (Offshore Mid-Norway: Integrated Margin and Basin Studies, 210429/E30) funded by the Norwegian Research Council through its Centre of Excellence (project 223272, Centre for Earth Evolution and Dynamics (CEED)). We thank R. Myklebust from TGS for providing the seismic data set and First Geo and TGS for providing the depth converted profile. We further thank L. Rüpke for his suggestions and comments on the reconstruction modelling, and Per Terje Osmundsen and Yuriy Maystrenko for their constructive and helpful reviews.

Tab. 1: Material properties of the crust, mantle, and stratigraphic layers

References

Abdelmalak, M.M., Andersen, T.B., Planke, S., Faleide, J.I., Corfu, F., Tegner, C., Shephard, G.E., Zastrozhnov, D., Myklebust, R., 2015. The ocean-continent transition in the mid-Norwegian margin: Insight from seismic data and an onshore Caledonian field analogue. Geology 43, 1011-1014.

Abdelmalak, M.M., Faleide, J.I., Planke, S., Gernigon, L., Zastrozhnov, D., Shephard, G.E., Myklebust, R., accepted. The T-Reflection and the deep crustal structure of the Vøring Margin: offshore Mid-Norway. Tectonics

Abdelmalak, M.M., Meyer, R., Planke, S., Faleide, J.I., Gernigon, L., Frieling, J., Sluijs, A., Reichart, G.J., Zastrozhnov, D., Theissen-Krah, S., Said, A., Myklebust, R., 2016a. Pre-breakup magmatism on the Vøring margin: Insight from new sub-basalt imaging and results from Ocean Drilling program hole 642E. Tectonophysics.

Abdelmalak, M.M., Planke, S., Faleide, J.I., Jerram, D.A., Zastrozhnov, D., Eide, S., Myklebust, R., 2016b. The development of volcanic sequences at rifted margins: New insights from the structure and morphology of the Vøring Escarpment, mid-Norwegian Margin. Journal of Geophysical Research: Solid Earth 121, 5212-5236.

Berndt, C., Planke, S., Alvestad, E., Tsikalas, F., Rasmussen, T., 2001. Seismic volcanostratigraphy of the Norwegian Margin: constraints on tectonomagmatic break-up processes. Journal of the Geological Society 158, 413-426.

Blystad, P., Brekke, H., Faerseth, R.B., Larsen, B.T., Skogseid, J., Tørudbakke, B., 1995. Structural Elements of the Norwegian Continental Shelf. Part II: The Norwegian Sea Region. Norwegian Petroleum Directorate Bulletin 8.

Breivik, A.J., Mjelde, R., Faleide, J.I., Murai, Y., 2006. Rates of continental breakup magmatism and seafloor spreading in the Norway Basin-Iceland plume interaction. Journal of Geophysical Research-Solid Earth 111.

Brekke, H., 2000. The tectonic evolution of the Norwegian Sea Continental Margin with emphasis on the Voring and More Basins, in: Nottvedt, A., Olaussen, S., Torudbakken, B., Gabrielsen, R.H., Brekke, H., Birkeland, O., Skogseid, J. (Eds.), Dynamics of the Norwegian margin. Geological Society, London, Special Publications, **167**, pp. 327-378.

Brune, S., Williams, S.E., Butterworth, N.P., Müller, R.D., 2016. Abrupt plate accelerations shape rifted continental margins. Nature advance online publication, 1-4.

Dore, A.G., Lundin, E.R., Fichler, C., Olesen, O., 1997. Patterns of basement structure and reactivation along the NE Atlantic margin. Journal of the Geological Society 154, 85-92.

Doré, A.G., Lundin, E.R., Jensen, L.N., Birkeland, O., Eliassen, P.E., Fichler, C., 1999. Principal tectonic events in the evolution of the northwest European Atlantic margin, in: Fleet, A.J., Boldy, S.A.R. (Eds.), Petroleum Geology of Northwest Europe: Proceedings of the 5th Conference. Geological Society, London, pp. 41-61.

Faerseth, R.B., Lien, T., 2002. Cretaceous evolution in the Norwegian Sea - a period characterized by tectonic quiescence. Marine and Petroleum Geology 19, 1005-1027.

Faleide, J.I., Tsikalas, F., Breivik, A.J., Mjelde, R., Ritzmann, O., Engen, O., Wilson, J., Eldholm, O., 2008. Structure and evolution of the continental margin off Norway and Barents Sea. Episodes 31, 82-91.

Gabrielsen, R.H., Odinsen, T., Grunnaleite, I., 1999. Structuring of the Northern Viking Graben and the More Basin; the influence of basement structural grain, and the particular role of the More-Trondelag Fault Complex. Marine and Petroleum Geology 16, 443-465.

Gaina, C., Gernigon, L., Ball, P., 2009. Palaeocene-Recent plate boundaries in the NE Atlantic and the formation of the Jan Mayen microcontinent. Journal of the Geological Society 166, 601-616.

Geoffroy, L., Burov, E.B., Werner, P., 2015. Volcanic passive margins: another way to break up continents. Sci Rep 5, 14828.

Gernigon, L., Blischke, A., Nasuti, A., Sand, M., 2015. Conjugate volcanic rifted margins, sea-floor spreading and microcontinent: Insights from new high-resolution aeromagnetic surveys in the Norway Basin. Tectonics, 907-933.

Gernigon, L., Gaina, C., Olesen, O., Ball, P.J., Péron-Pinvidic, G., Yamasaki, T., 2012. The Norway Basin revisited: From continental breakup to spreading ridge extinction. Marine and Petroleum Geology 35, 1-19.

Gernigon, L., Lucazeau, F., Brigaud, F., Ringenbach, J.C., Planke, S., Le Gall, B., 2006. A moderate melting model for the Voring margin (Norway) based on structural observations and a thermo-kinematical modelling: Implication for the meaning of the lower crustal bodies. Tectonophysics 412, 255-278.

Gernigon, L., Ringenbach, J.C., Planke, S., Le Gall, B., 2004. Deep structures and breakup along volcanic rifted margins: insights from integrated studies along the outer Voring Basin (Norway). Marine and Petroleum Geology 21, 363-372.

Gernigon, L., Ringenbach, J.C., Planke, S., Le Gall, B., Jonquet-Kolsto, H., 2003. Extension, crustal structure and magmatism at the outer Voring Basin, Norwegian margin. Journal of the Geological Society 160, 197-208.

Gomez, M., Verges, J., Fernandez, M., Torne, M., Ayala, C., Wheeler, W., Karpuz, R., 2004. Extensional geometry of the mid Norwegian Margin before Early Tertiary continental breakup. Marine and Petroleum Geology 21, 177-194.

Grunnaleite, I., Gabrielsen, R.H., 1995. Structure of the More Basin, mid-Norway continental margin. Tectonophysics 252, 221-251.

Kvarven, T., Ebbing, J., Mjelde, R., Faleide, J.I., Libak, A., Thybo, H., Flueh, E.R., Murai, Y., 2014. Crustal structure across the Møre margin, mid-Norway, from wide-angle seismic and gravity data. Tectonophysics 626, 21-40.

Lavier, L.L., Manatschal, G., 2006. A mechanism to thin the continental lithosphere at magma-poor margins. Nature 440, 324-328.

Lundin, E., Dore, A.G., 2002. Mid-Cenozoic post-breakup deformation in the 'passive' margins bordering the Norwegian-Greenland Sea. Marine and Petroleum Geology 19, 79-93.

Lundin, E.R., Dore, A.G., 1997. A tectonic model for the Norwegian passive margin with implications for the NE Atlantic: Early Cretaceous to break-up. Journal of the Geological Society 154, 545-550.

Lundin, E.R., Dore, A.G., 2011. Hyperextension, serpentinization, and weakening: A new paradigm for rifted margin compressional deformation. Geology 39, 347-350.

Mjelde, R., Raum, T., Kandilarov, A., Murai, Y., Takanami, T., 2009. Crustal structure and evolution of the outer More Margin, NE Atlantic. Tectonophysics 468, 224-243.

Mosar, J., Eide, E.A., Osmundsen, P.T., Sommaruga, A., Torsvik, T.H., 2002. Greenland - Norway separation: A geodynamic model for the North Atlantic. Norwegian Journal of Geology 82, 281-298.

Nirrengarten, M., Gernigon, L., Manatschal, G., 2014. Lower crustal bodies in the More volcanic rifted margin: Geophysical determination and geological implications. Tectonophysics 636, 143-157.

Olafsson, I., Sundvor, E., Eldholm, O., Grue, K., 1992. Møre Margin: Crustal structure from analysis of Expanded Spread Profiles. Marine Geophysical Researches 14, 137-162.

Osmundsen, P.T., Ebbing, J., 2008. Styles of extension offshore mid-Norway and implications for mechanisms of crustal thinning at passive margins. Tectonics 27.

Perez-Gussinye, M., Reston, T.J., Phipps Morgan, J., 2001. Serpentinization and magmatism during extension at non-volcanic margins: the effect of initial lithospheric structure. Geological Society, London, Special Publications 187, 551-576.

Peron-Pinvidic, G., Manatschal, G., Osmundsen, P.T., 2013. Structural comparison of archetypal Atlantic rifted margins: A review of observations and concepts. Marine and Petroleum Geology 43, 21-47.

Planke, S., T., R., Rey, S.S., Myklebust, R., 2005. Seismic characteristics and distribution of volcanic intrusions and hydrothermal vent complexes in the Vøring and Møre basins. Geological Society, London, Petroleum Geology Conference series 6, 833-844.

Ranero, C.R., Perez-Gussinye, M., 2010. Sequential faulting explains the asymmetry and extension discrepancy of conjugate margins. Nature 468, 294-U180.

Reemst, P., Cloetingh, S., 2000. Polyphase rift evolution of the Voring margin (mid-Norway): Constraints from forward tectonostratigraphic modeling. Tectonics 19, 225-240.

Ren, S.C., Faleide, J.I., Eldholm, O., Skogseid, J., Gradstein, F., 2003. Late Cretaceous-Paleocene tectonic development of the NW Voring Basin. Marine and Petroleum Geology 20, 177-206.

Ren, S.C., Skogseid, J., Eldholm, O., 1998. Late Cretaceous-Paleocene extension on the Voring Volcanic Margin. Marine Geophysical Researches 20, 343-369.

Reynisson, R.F., Ebbing, J., Lundin, E., Osmundsen, P.T., 2010. Properties and distribution of lower crustal bodies on the mid-Norwegian margin, pp. 843-854.

Roberts, A.M., Corfield, R.I., Kusznir, N.J., Matthews, S.J., Hansen, E.K., Hooper, R.J., 2009. Mapping palaeostructure and palaeobathymetry along the Norwegian Atlantic continental margin: More and Voring basins. Petroleum Geoscience 15, 27-43.

Rüpke, L.H., Schmalholz, S.M., Schmid, D.W., Podladchikov, Y.Y., 2008. Automated thermotectonostratigraphic basin reconstruction: Viking Graben case study. AAPG Bulletin 92, 309-326.

Rüpke, L.H., Schmid, D.W., Perez-Gussinye, M., Hartz, E., 2013. Interrelation between rifting, faulting, sedimentation, and mantle serpentinization during continental margin formation—including examples from the Norwegian Sea. Geochemistry, Geophysics, Geosystems, 4351-4369.

Scheck-Wenderoth, M., Maystrenko, Y., 2008. How warm are passive continental margins? A 3-D lithosphere-scale study from the Norwegian margin. Geology 36, 419-422.

Scheck-Wenderoth, M., Raum, T., Faleide, J.I., Wjelde, R., Horsfield, B., 2007. The transition from the continent to the ocean: a deeper view on the Norwegian margin. Journal of the Geological Society 164, 855-868.

Skogseid, J., 1994. Dimensions of the Late Cretaceous Paleocene Northeast Atlantic Rift Derived from Cenozoic Subsidence. Tectonophysics 240, 225-247.

Skogseid, J., Planke, S., Faleide, J.I., Pedersen, T., Eldholm, O., Neverdal, F., 2000. NE Atlantic continental rifting and volcanic margin formation, in: Nottvedt, A., Larsen, B.T., Gabrielsen, R.H., Olaussen, S., Torudbakken, B., Skogseid, J., Brekke, H., Birkeland, O. (Eds.), Dynamics of the Norwegian Margin. Geological Society , London, Special Publications, **167**, pp. 295-326.

Steckler, M.S., Watts, A.B., 1978. SUBSIDENCE OF ATLANTIC-TYPE CONTINENTAL-MARGIN OFF NEW-YORK. Earth and Planetary Science Letters 41, 1-13.

Stewart, J., Watts, A.B., Bagguley, J.G., 2000. Three-dimensional subsidence analysis and gravity modelling of the continental margin offshore Namibia. Geophys. J. Int. 141, 724-746.

Sweeney, J.J., Burnham, A.K., 1990. Evaluation of a Simple Model of Vitrinite Reflectance Based on Chemical Kinetics. AAPG Bull.-Am. Assoc. Petr. Geol. 74, 1559-1570.

Talwani, M., Eldholm, O., 1972. Continental Margin off Norway: A Geophysical Study. Geol. Soc. Am. Bull. 83, 3575-3606.

Talwani, M., Worzel, J.L., Landisman, M., 1959. Rapid Gravity Computations for 2-Dimensional Bodies with Application to the Mendocino Submarine Fracture Zone. Journal of Geophysical Research 64, 49-59.

The International Gravimetric Bureau, 2012. IAG Geodesist's Handbook - Journal of Geodesy. Springer, pp. 787-974.

Theissen, S., Rüpke, L.H., 2010. Feedbacks of sedimentation on crustal heat flow: New insights from the Voring Basin, Norwegian Sea. Basin Research 22, 976-990.

Torsvik, T.H., Cocks, L.R.M., 2005. Norway in space and time: A Centennial cavalcade. Norwegian Journal of Geology 85, 73-86.

Torsvik, T.H., Van der Voo, R., Meert, J.G., Mosar, J., Walderhaug, H.J., 2001. Reconstructions of the continents around the North Atlantic at about the 60th parallel. Earth and Planetary Science Letters 187, 55-69.

Tsikalas, F., Faleide, J.I., Eldholm, O., Antonio Blaich, O., 2012. 5 - The NE Atlantic conjugate margins, Regional Geology and Tectonics: Phanerozoic Passive Margins, Cratonic Basins and Global Tectonic Maps. Elsevier, Boston, pp. 140-201.

Wangen, M., 1995. The blanketing effect in sedimentary basins. Basin Research 7, 283-298.

Wangen, M., Faleide, J.I., 2008. Estimation of crustal thinning by accounting for stretching and thinning of the sedimentary basin -- An example from the Vøring margin, NE Atlantic. Tectonophysics 457, 224-238.

Wangen, M., Mjelde, R., Faleide, J.I., 2011. Modelling thermal transients from magmatic underplating-an example from the Voring margin (NE Atlantic). Computational Geosciences 15, 771-788.

White, R., McKenzie, D., 1989. Magmatism at rift zones: The generation of volcanic continental margins and flood basalts. Journal of Geophysical Research: Solid Earth 94, 7685-7729.

Won, I.J., Bevis, M., 1987. Computing the Gravitational and Magnetic-Anomalies Due to a Polygon - Algorithms and Fortran Subroutines. Geophysics 52, 232-238.

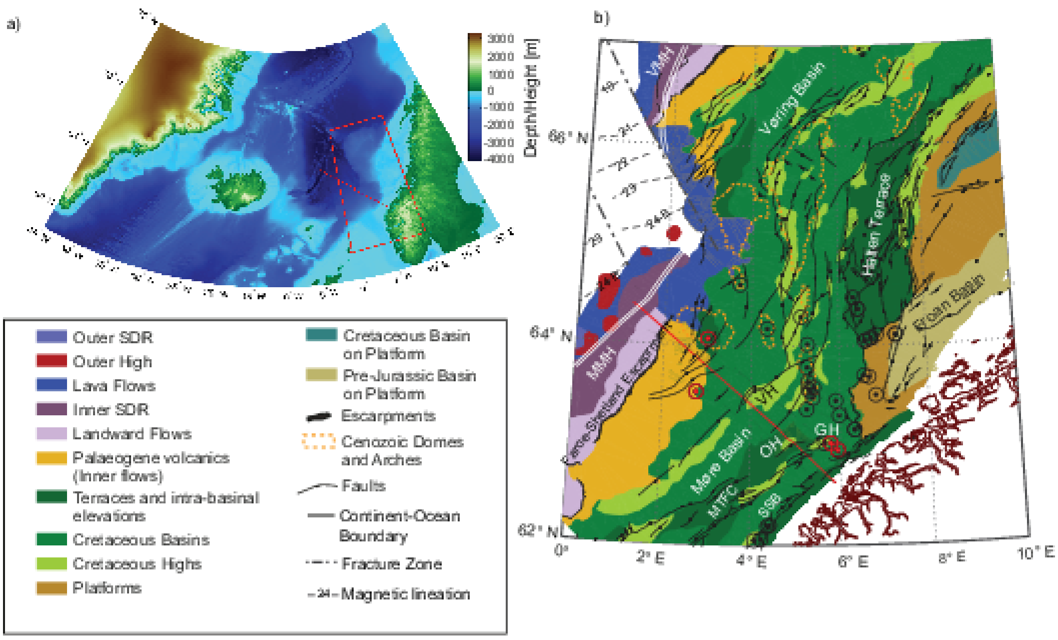

Fig. 1: a) Bathymetry and topography map showing the study area. The red lines indicate the seismic lines used for the structural reconstruction; the red frame marks the location of 1b). b) Close up of the study area including main structural features in the Møre Margin. Seismic profiles used for the reconstruction study in red. Black dots indicate well locations in the area and the wells projected onto the key profile are marked in red. GH = Gossa High, MMH = Møre Marginal High, OH = Ona High, MTFC = Møre-Trøndelag Fault Complex, SSB = Slørebotn Sub-basin, VH = Vigra High, VMH = Vøring Marginal High. Interpretation of volcanic facies units are taken from Abdelmalak et al. (2015; 2016b).

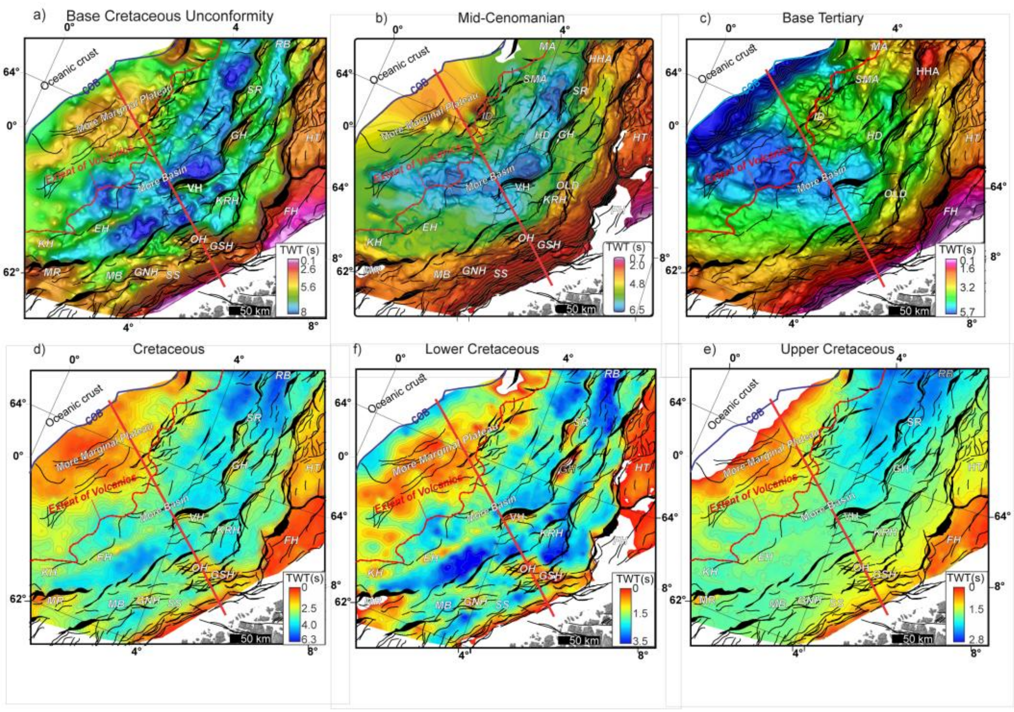

Fig. 2: Top (a-c) row shows time-structure maps of the Cretaceous units. Time-thickness maps are plotted at the bottom (d-f). The blue and red lines mark the continent ocean boundary (COB) and the extent of the volcanics, respectively. The COB is defined as seaward termination of the K-reflector (Abdelmalak et al., 2016a) The thick red line shows the location of the key profile. EH = Ervik High; FH = Frøya High; GH = Grip High; GNH = Gnausen High; GSH = Gossa High; HD = Havsule Dome; HHA = Helland-Hansen Arch; HT = Halten Terrace; ID = Isak Dome; KH = Kinn High; KRH = Kiran High; MA = Modgunn Arch; MB = Marulk Basin; MR = Manet Ridge; OH = Ona High; OLD = Ormen Lange Dome; RB = Rås Basin; SMA = Southern Modgunn Arch; SR = Slettringen Ridge; SS = Slørebotn Subbasin; VH = Vigra High

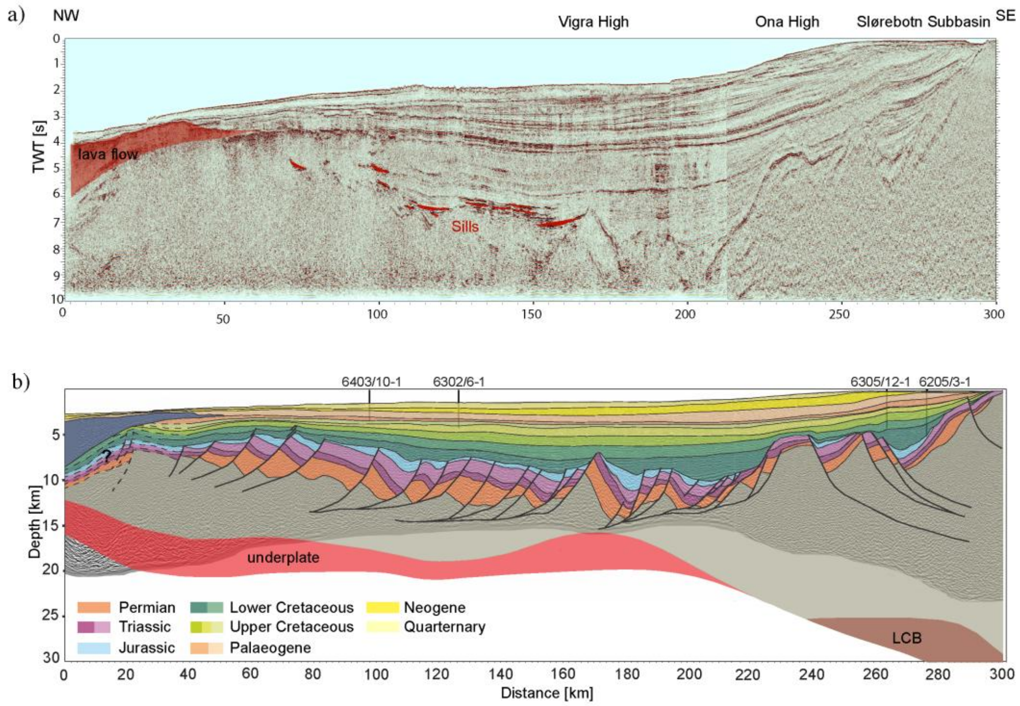

Fig. 3: a) Seismic reflection of the Møre transect (red line in Fig. 1B). The red area in the western part indicates the breakup lave flows. b) Geological interpretation of a). The question mark and dashed lines show the locations where the interpretation of the pre mid-Cretaceous strata are difficult and uncertain due to the widespread sill intrusions.

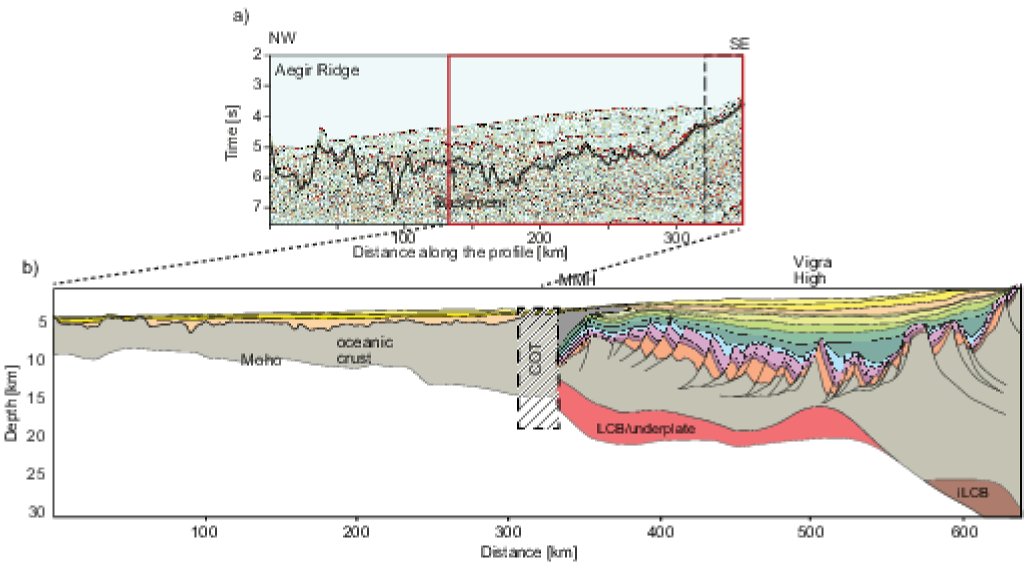

Fig. 4: A) Seismic line LOS 99-002 with interpretation of basement from (Breivik et al., 2006).

b) Combined transect including sediments overlying oceanic crust. This transect is the stratigraphy input for the second part of the reconstruction study.

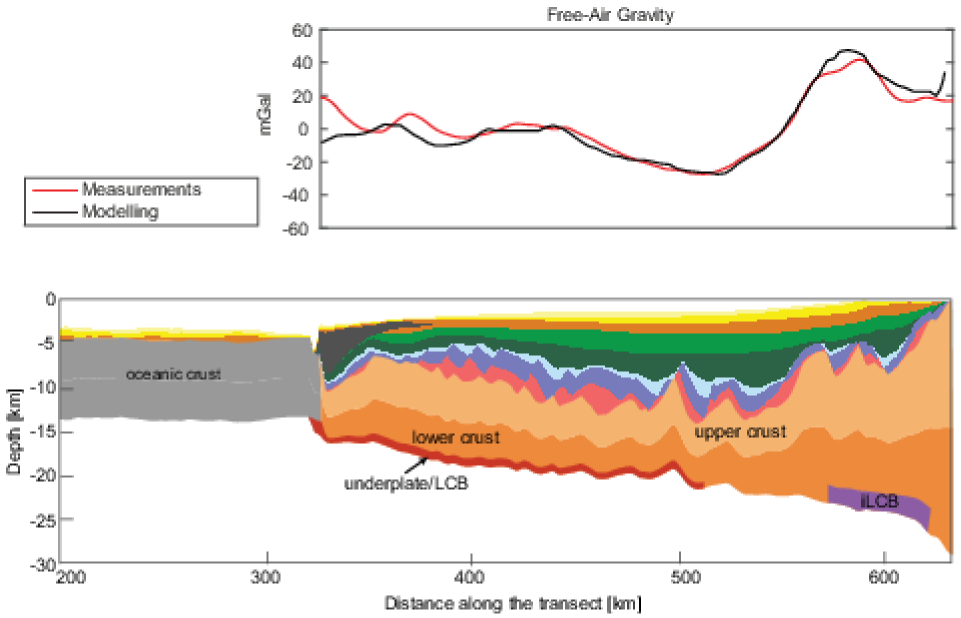

Fig. 5: Crustal configuration after basin reconstruction and gravity comparison. a) The modelled (black line) free-air gravity anomaly fits well the measured data (red line). b) Resulting crustal thickness and stratigraphy of the reconstructed transect with total initial crustal thickness of 32 km. The locations of the inner and outer LCBs are constrained by gravity comparison and implemented as initial heterogeneities that change the density distribution of the crust.

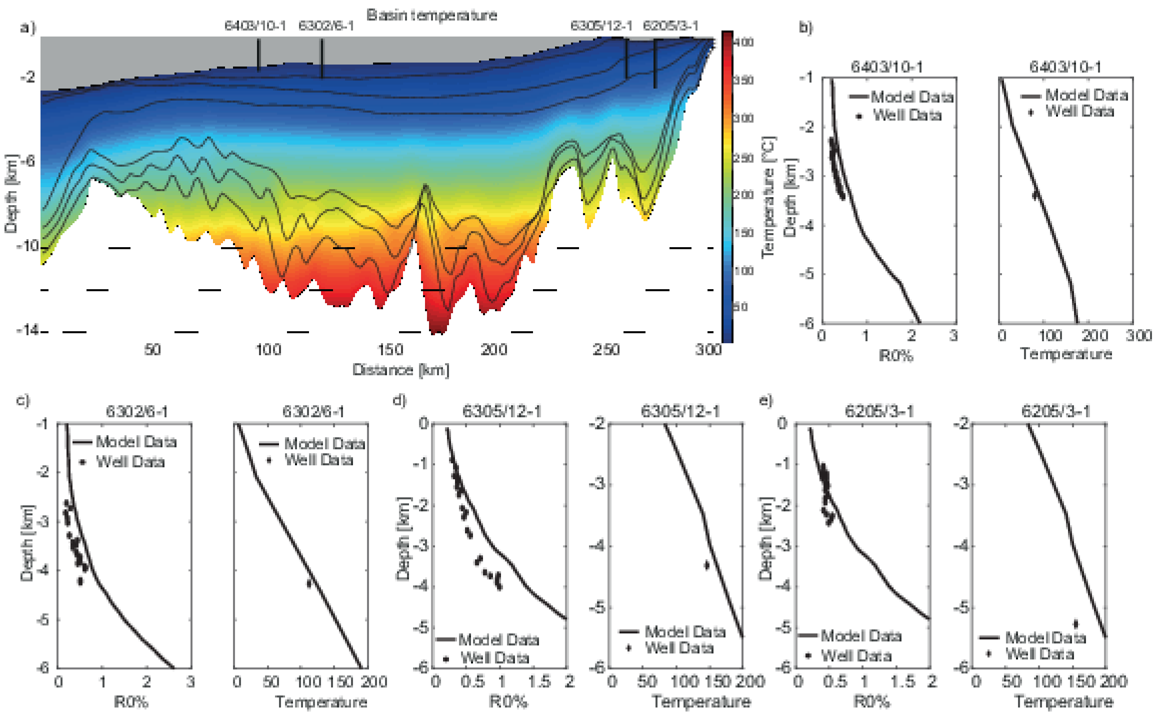

Fig. 6: Basin temperature and comparison of observed and modelled data for the four wells projected onto the transect (Fig. 5). The top left figure (a) shows the modelled basin temperature and the period boundaries (black lines) from Quaternary to Triassic. The left plot of each well (b-e) shows observed (dots) and modelled (solid line) vitrinite reflectance (Easy Ro%). Temperature comparison is shown in the right panels. Modelled values are displayed as black line and observed data as diamonds.

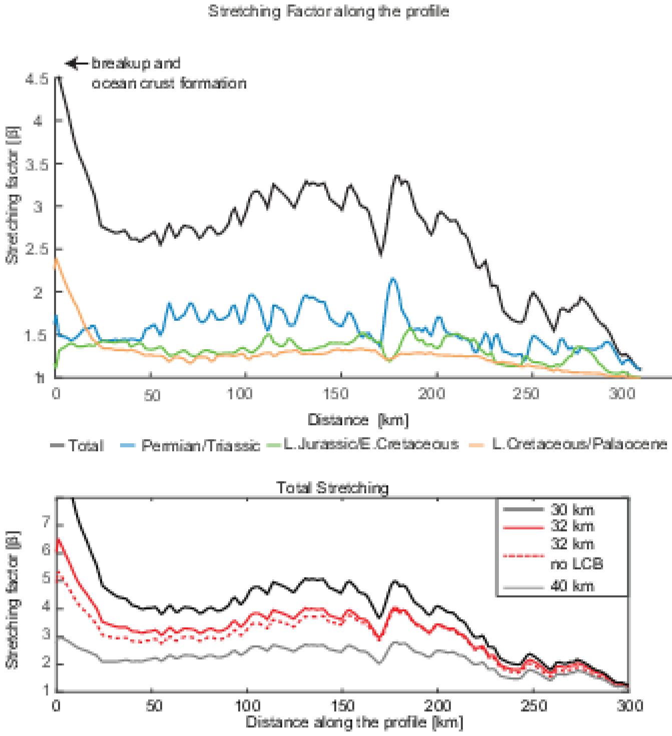

Fig. 7: a) Total stretching and stretching factors for each rift phase along the transect for a setup with 35 km initial crustal thickness. Most thinning occurred prior to the final rifting which accounts for ~35% of total stretching. Highest stretching occurs at the depocenters. b) Comparison of total stretching factor from structural reconstruction for 30 (black line), 32 (red lines) and 40 km (grey line) initial crustal thickness. Higher stretching factors are needed if a LCB is considered in the reconstruction modelling.

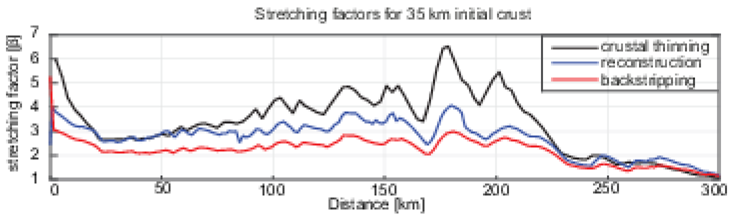

Fig. 8: A comparison of stretching factors calculated with different methods for 35 km initial crust is shown. The comparison is calculated for the central Møre Basin only without breakup. The classical backstripping method results in lower stretching factors compared to the reconstruction due to the underestimation of sedimentation. See text for discussion.

Table 1

		Matrix Density (kg m^{-3})	Thermal Expansion (K^{-1})	Radiogenic Heat (W m^{-3})	Conductivity (W $m^{-1}K^{-1}$)	Heat capacity ($Jkg^{-1}K^{-1}$)	Surface Porosity (%)	Compaction length (km^{-1})
Mantle	Peridotite	3340	3.2 x 10^{-5}	0	3.5	1000		
Lower Crust	Diabase	2850	2.4 x 10^{-5}	1.8 x10^{-7}	2.6	800		
Upper Crust	Granite	2750	2.4 x 10^{-5}	2 x10^{-6}	2.6	800		
Quarternary	Sandstone	2650		7 x10^{-7}	3.95	855	41	0.31
Neogene	Sandstone	2700		7 x10^{-7}	3.95	855	41	0.31
Palaeogene	Shale	2700		2 x10^{-6}	1.64	860	70	0.83
Upper Cretaceous	organic rich Shale	2610		2 x10^{-6}	1.54	880	70	0.83
Lower Cretaceous	Shale	2700		2 x10^{-6}	1.64	860	70	0.83
Upper Jurassic	Sandstone	2720		7 x10^{-7}	3.95	855	41	0.31
Lower Jurassic	Marl	2700		1 x10^{-6}	2	850	50	0.5
Triassic	Siltstone	2710		1 x10^{-6}	2.01	940	55	0.51
Permian	sandy Shale	2700		1.71 x10^{-6}	1.84	860	65	0.83
inner LCB		3300	2.4 x 10^{-5}	1.8 x10^{-7}	2.6	800		
outer LCB/magmatic underplate		3100	2.4 x 10^{-5}	0	2.6	1000		

Highlights

- New and reprocessed seismic data improved structural mapping at the Møre Margin
- Time-structure and thickness maps of the Cretaceous units have been constructed
- Stratigraphy reconstruction of a transect reveals 188 km extension
- Average stretching factor is 2.2-3.6 depending on assumed initial crustal thickness